Biotechnology and Bioprocess Engineering
https://doi.org/10.1007/s12257-024-00146-x

RESEARCH PAPER

Assessing the applicability of tunicate skin-extracted cellulose as a base material for ultrasound gel

Ji Woo Han[1] · Nu Ri Han[1] · Hye Jin Hwang[2] · Byung Man Lee[2] · Hwa Sung Shin[2,3] · Sang Hyun Lee[1] · Yun Jung Yang[2,3]

Received: 16 June 2024 / Revised: 16 August 2024 / Accepted: 19 August 2024

Abstract

Cellulose is widely considered an outstanding biomaterial due to its remarkable ionic properties, exceptional biocompatibility, and low toxicity. Its abundant surface hydroxyl groups facilitate increased hydrogen bonding, improving gelation and swelling capabilities. Moreover, incorporating carboxymethyl groups enhances solubility and allows for diverse formulations, serving as multifunctional cross-linkers. Among the various sources of this compound, tunicate-derived cellulose is an animal-derived cellulose and food byproduct with low utility. However, recycling tunicate skin into a useful biomaterial would provide access to the unique characteristics of animal cellulose, distinct from those of plant-derived cellulose. Particularly, tunicate cellulose has a longer fiber length than plant cellulose, enhancing the sound propagation speed within the material and making it suitable for the production of ultrasound-responsive gels. This study examined the viscosity and conductivity of tunicate-derived carboxymethyl celluloseto assess its applicability as an ultrasound gel. Additionally, small molecule release after ultrasound stimulation was also evaluated.

Keywords Tunicate · By-product · Carboxymethyl cellulose · Ultrasound gel

1 Introduction

Cellulose is a naturally occurring anionic polysaccharide composed of a linear chain of D-glucose molecules linked by β-1,4-glycosidic bonds [25, 30]. Due to its minimal toxicity and allergenicity, cellulose has been widely used as a biocompatible biomaterial [26]. Furthermore, cellulose can be modified into diverse structures by substituting groups such as alkyl, carboxymethyl, and alkene for the hydroxyl group.

Among various sources of cellulose, the non-edible byproduct of tunicate skin (TS) constitutes a promising candidate for engineering applications because it contains a high percentage of cellulose (60%) compared to plant cellulose (30%–50%) [38]. The remaining ~ 40% of TS is primarily protein, with typical impurities such as lignin and hemicellulose [33]. Therefore, tunicate cellulose (TC) is of higher purity than plant-derived cellulose. In South Korea alone, up to 31,326 tons of TS waste are generated annually, creating significant disposal and environmental issues [38]. TC, derived from animals, differs from plant- and bacteria-derived cellulose. Its higher crystallinity index (CrI) (> 0.8) compared to plants (0.74) and bacteria (0.3) indicates a greater alignment of fibers in TC [5, 33, 57]. Specifically, the crystallinity of TC ranges from 85 to 99%, depending on the developmental stage (larval or adult). Its aspect ratio of approximately 80 surpasses that of plant-derived cellulose (~ 10) [32, 33, 56]. This high crystallinity and aspect ratio result in larger nanocrystals with greater thermal stability (TC: 335 °C; plant

Ji Woo Han, Nu Ri Han, Hye Jin Hwang, and Byung Man Lee have contributed equally to this work.

✉ Hwa Sung Shin
hsshin@inha.ac.kr

✉ Sang Hyun Lee
sanghlee@konkuk.ac.kr

✉ Yun Jung Yang
yj.yang@inha.ac.kr

[1] Department of Biological Engineering, Konkuk University, Seoul 05029, Korea

[2] Department of Biological Engineering, Inha University, Incheon 22212, Korea

[3] Department of Biological Sciences and Bioengineering, Inha University, Incheon 22212, Korea

Published online: 19 September 2024

cellulose: 200–300 °C) [5, 33, 57]. However, high crystallinity also poses challenges, as it makes cellulose less soluble, requiring harsh conditions such as homogenizers or sulfuric acid solutions to promote dissolution. Carboxymethyl groups are commonly introduced to cellulose to address these limitations to increase its solubility and conductivity [12, 21].

Although many external stimuli (ions, pH, light, temperature, etc.) have been proposed as potential drug delivery systems, ultrasound-assisted methods have recently garnered increasing attention as promising agents for the delivery of therapeutic compounds, genetic materials, hormones, and proteins due to their cavitation activity [1, 28, 41]. Cavitation exerts a physical impact that aids in releasing biomolecules and cells while also disrupting the stratum corneum to facilitate the transportation of large molecules.

This study leverages the advantages of TC-based hydrogel to maintain gel pH and viscosity across various temperatures. Additionally, incorporating TC enhances the gel's conductivity, improving the transmission of ultrasound signals between the device and the skin. Collectively, our findings demonstrated that the generated TC gel possesses a superior capability for molecular release under ultrasound stimulation, highlighting its potential as an efficient delivery material, especially for the ultrasound gel.

2 Materials and methods

2.1 TC extraction

The TS were cut into 1 cm × 1 cm pieces and soaked in 70% (v/v) ethyl alcohol (Duksan) for 24 h before being freeze-dried. The freeze-dried TS was heated at 80 °C in 5% (v/v) sodium hydroxide (NaOH, Samchun) for 24 h to remove residual protein. Acid washing and bleaching were carried out in a 5 L fermenter (Marado-PDA, Bionics) containing 7% (v/v) hydrogen chloride (HCl, Samchun) for 24 h, followed by treatment with 4% (v/v) hydrogen peroxide (H_2O_2, Samchun). This mixture was stirred for 4 h at 80 °C, and the processed TC was then dried at room temperature.

The cellulose content in TS was analyzed by determining structural carbohydrates and lignin biomass according to laboratory analytical procedures [50]. The TC was treated with 72% (v/v) sulfuric acid (H_2SO_4, Samchun) at 30 °C for 2 h, followed by treatment with dilute acid (4% (v/v)) at 121 °C for 1 h. The hydrolysis products were determined using high-performance liquid chromatography (HPLC, Shimadzu CBM-40) equipped with an RI detector and a Shodex SP0810 column (Resonac) operated at 85 °C. The mobile phase consisted of deionized water (DW) at a 0.6 mL/min flow rate.

The molecular weights (MW) and degrees of polymerization (DP) of purified TC were determined by gel permeation chromatography (GPC, Agilent 1200S/mini DAWN TREOS) using tetrahydrofuran as a solvent. The TC sample was derivatized with phenyl isocyanate to be dissolved in tetrahydrofuran (Sigma-Aldrich) [27]. To this end, 4 mL of 99.8% (v/v) anhydrous pyridine (Sigma-Aldrich) and 0.5 mL of 98% (v/v) phenyl isocyanate (Kanto Chemical Co.) were added to 15 mg of TC, and the vial was sealed with a Teflon-coated cap. The vial was kept in an oil bath at 70 °C and stirred continuously for 72 h to complete the reaction. The reaction was then stopped by adding 1 mL of methyl alcohol. Subsequently, the resulting mixture was slowly added to 70% (v/v) methyl alcohol (Duksan) to promote precipitation of the derivatized TC. Next, the solid products were collected by filtration, washed with 70% (v/v) methyl alcohol (Duksan), and then washed twice with DW. Ginallt, the thoroughly washed derivatized TC was dried overnight at 65 °C.

2.2 Synthesis of tunicate carboxymethyl cellulose (TCMC)

The purified TC was functionalized into carboxymethyl cellulose (CMC) through homogeneous carboxymethylation using lithium perchlorate ($LiClO_4 \bullet 3H_2O$, Alfa Aesar) as described in a previous study [14] with slight modifications. The TC was stirred with $LiClO_4 \bullet 3H_2O$ (1% (w/v)) (Alfa Aesar) and heated to 100 °C in a closed round flask with a magnetic stirrer until the TC was completely dissolved. Sodium hydroxide (0.06% (w/v)) (NaOH, Samchun) and sodium chloroacetate (0.048% (w/v)) (Thermo Fisher Scientific) were then added to the mixture in a stepwise manner, and the reaction was carried out at 100 °C for 1 h. The product was precipitated in methanol, and the recovered precipitate was re-dissolved in 10 mL of DW. The dissolved product was neutralized with acetic acid (Duksan) and re-precipitated with ethyl alcohol. The purification steps were repeated three times, and the final product was dried at room temperature and labeled as TCMC.

2.3 Physicochemical characterization of TCMC

Changes in functional groups in the TCMC were investigated using Fourier-transform infrared spectroscopy (FT-IR). The dried TC and TCMC were ground using a homogenizer, and their FT-IR spectra were determined by averaging 16 scans per spectrum at a 600–2000 cm^{-1} range (resolution, 4 cm^{-1}; scanning interval, 1 cm^{-1}) using an FT/IR-4100 type A spectrometer (Jasco International Co. Ltd.).

HPLC analyses were conducted to examine the degree of substitution (DS) of TCMC [44]. To hydrolyze TCMC, 0.1 g of TCMC was dispersed in 2 mL of 70% (v/v) perchloric acid ($HClO_4$, Samchun) for 10 min at 25 °C. After the first hydrolysis reaction, the mixture was diluted with 18 mL DW and then incubated at 100 °C for 16 h for additional hydrolysis. After the second hydrolysis reaction, the mixture was

cooled to room temperature, neutralized with 2 M potassium hydroxide (KOH, Samchun), and then kept at 4 °C for 1 h to complete the potassium perchlorate ($KClO_4$) precipitation. The precipitated sample was filtered with a 0.2 µm cellulose acetate filter and washed three times with DW. The filtrate was evaporated until the sample volume decreased. The diluted sample was then filtered with a 0.2 µm PVDF filter and used for HPLC analysis. The contents of carboxymethylated glucoses in hydrolyzed TCMC samples were analyzed using HPLC (CBM-40, Shimadzu) equipped with an RI detector and an Aminex HPX-87H column operated at 65 °C. The mobile phase consisted of 5 mM sulfuric acid with a 0.5 mL/min flow rate. The DS of TCMC was calculated as follows:

$$DS = 3x_t + 2x_d + x_m$$

where x_t, x_d, and x_m are the mole fraction of tri-carboxylated, di-carboxylated, and mono-carboxylated glucose, respectively.

The X-ray diffraction (XRD) patterns of TC and TCMC were analyzed using an X-ray diffractometer (Smartlab, Rigaku). The samples were scanned in a 2 theta (θ) range of 2–40° at 40 kV and 40 mA. The CrI of cellulose was calculated using the height difference method [45].

2.4 Viscosity, pH, and conductivity measurement of TCMC gel

Viscosity measurements for the TCMC gels were conducted using a viscometer (DV2T, Brookfield) equipped with a plate-shaped spindle (CPA-52Z). The TCMC gels were carefully placed on the cone plate, and the gap between the spindle and the plate was adjusted accordingly. The shear speed was set at 1 rpm for 30 s to ensure consistency, and the temperature was maintained at a constant 25 °C. The viscosity values presented on the graph are denoted in poise (P).

Both pH (Ino lab) and conductivity (BANTE Instruments) were measured under different temperatures (4 °C, 23 °C, and 50 °C). A gel containing only carbopol, triethanolamine, and glycerin without TC was used as the negative control and labeled 'base gel.' The ratios of carbopol, triethanolamine, and glycerin in each sample were denoted as numbers after the letters C (carbopol), T (triethanolamine), and G (glycerin).These properties were compared with those of a commercially available gel (Ecosonic, Senipia).

2.5 Ultrasound-induced dye release of TCMC gel

Brilliant blue (Sigma-Aldrich) was added at the initial stage of ultrasound gel mixing. The gel was then washed to remove any uncaptured dye. An ultrasound device with a facial care instrument charger (Protec) was applied to the gel for 15 min. The released dye was measured at 550 nm using a microplate reader (BioTek) every minute for the duration of the application.

3 Results and discussion

3.1 Purification of TC from TS

TC was extracted from TS, after which the cellulose and protein content were measured. The cellulose content was determined using HPLC, the standard method for determining carbohydrates, which calculates it as glucose multiplied by the conversion factor of 0.9. The initial cellulose content in TS was 44.2%, and the purification process successfully reduced the protein content while increasing the cellulose content. Following the deproteination process, the cellulose content of the TS sample increased to 76.6%. The acid-washing process further elevated the cellulose content to 96.3%. Ultimately, TC obtained through the H_2O_2 bleaching process displayed a cellulose content of over 99%, with protein and ash contents being undetectable (less than 0.01%) (Fig. 1A).

The number-average MW (M_n) and weight-average MW (M_W) of purified TC, as determined by GPC, were 164,606 and 1,563,427, respectively. The polydispersity index (PDI), calculated by dividing M_w by M_n, was 9.50. The number-average DP (DP_n) and weight-average DP (DP_w) were obtained by dividing M_n and M_w by 519 g/mol, representing the MW of the tricarbanilated cellulose unit [16]. For TC, the DP_n and DP_w of TC were 317 and 3012, respectively. The DP values of purified TC exceeded those of various cellulose types, including delignified wood pulp, cotton linter pulp, and bacterial cellulose [6].

3.2 The characterization of TCMC

Carboxymethylation of TC was performed to enhance its hydrophilicity using various classical heterogeneous and homogeneous carboxymethylation methods [50]. However, only the homogeneous carboxymethylation method employing lithium perchlorate successfully yielded water-miscible TCMC. More than 10% (w/v) of TCMC could be fully dissolved in water. The TCMC gel was further formulated with the mix of carbopol, triethanolamine, and glycerin (Fig. 1B).

Changes in the functional groups of TCMC were verified by FT-IR (Fig. 2A). Peaks evident in TC and TCMC were observed at 2939 and 3332 cm^{-1}, ascribed to –CH and –OH groups, respectively. Unique bands exclusively present in TCMC appeared at 1594 and 1417 cm^{-1}, indicating the presence of carboxylate anions ($–COO^-$) and scissoring/bending vibrations of $–CH_2$ groups. These findings support the existence of carboxymethyl substituents [14, 27]. Specific peaks displayed shifts due to carboxymethylation. The FT-IR

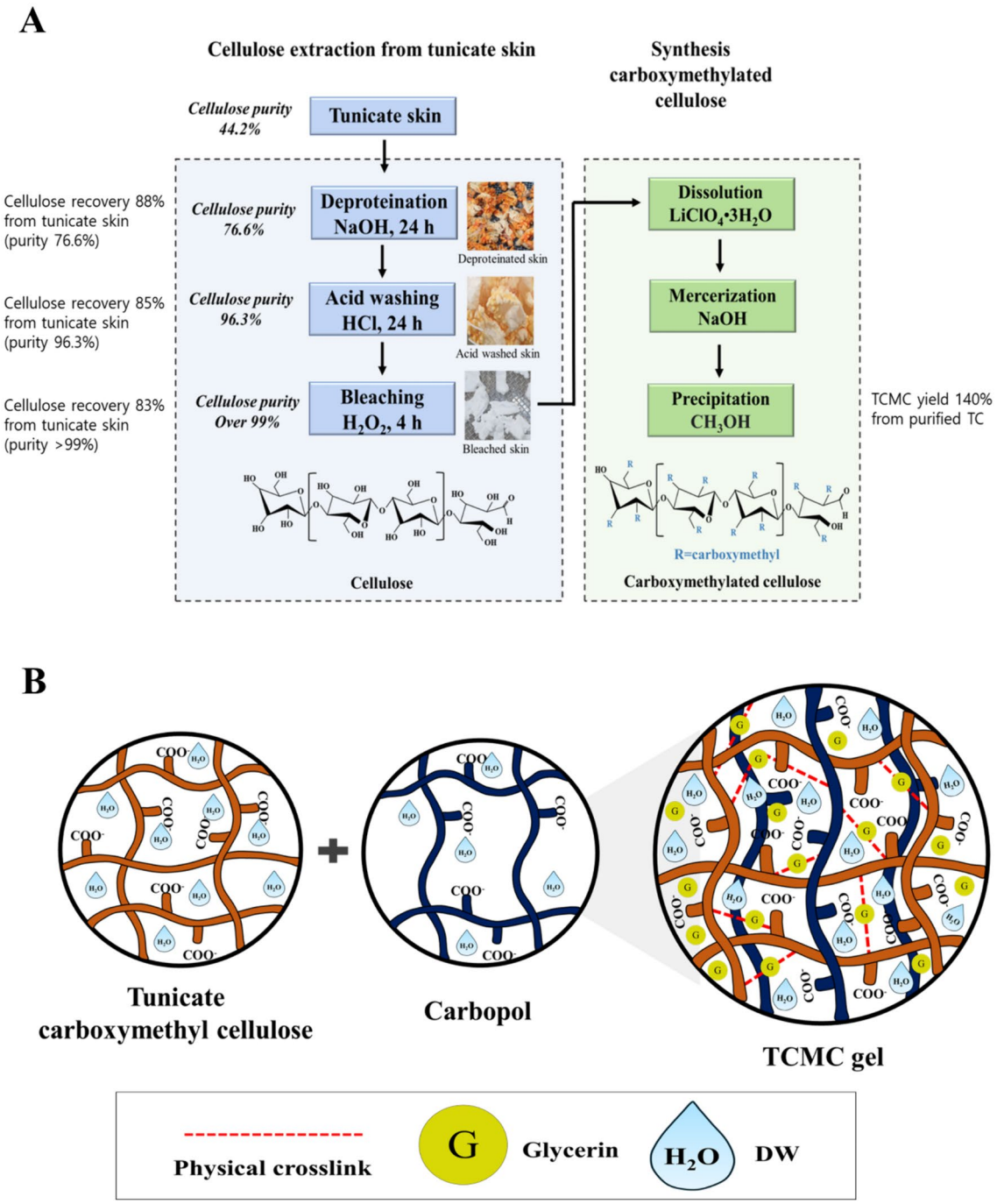

Fig. 1 **A** Extraction and synthesis process of TCMC. **B** TCMC gel network. TCMC: tunicate carboxymethyl cellulose, DW: deionized water

spectrum band of TC at 1052 cm^{-1} shifted to 1061 cm^{-1}, whereas the peak at 1031 cm^{-1} shifted to 1026 cm^{-1}. Both shifts were attributed to β-(1,4)-glycosidic linkages between the carboxymethylated and unmodified glucose units [14].

The DS of TCMC was measured through the HPLC (Fig. 2B). The mole fractions of glucose, 2-; 3- and 6-mono-*O*-carboxymethyl glucose (x_m), 2,3-; 2,6- and 3,6-di-*O*-carboxymethyl glucose (x_d), and 2,3,6-tri-*O*-carboxymethyl glucose (x_t) in hydrolyzed TCMC samples were 0.14, 0.38, 0.36, and 0.12, respectively (Fig. 2B). The calculated DS of TCMC was 1.46. These findings unambiguously demonstrate the successful carboxymethylation of TC through homogeneous carboxymethylation using lithium perchlorate. The significant water solubility of TCMC can be attributed to the presence of highly substituted carboxymethyl groups.

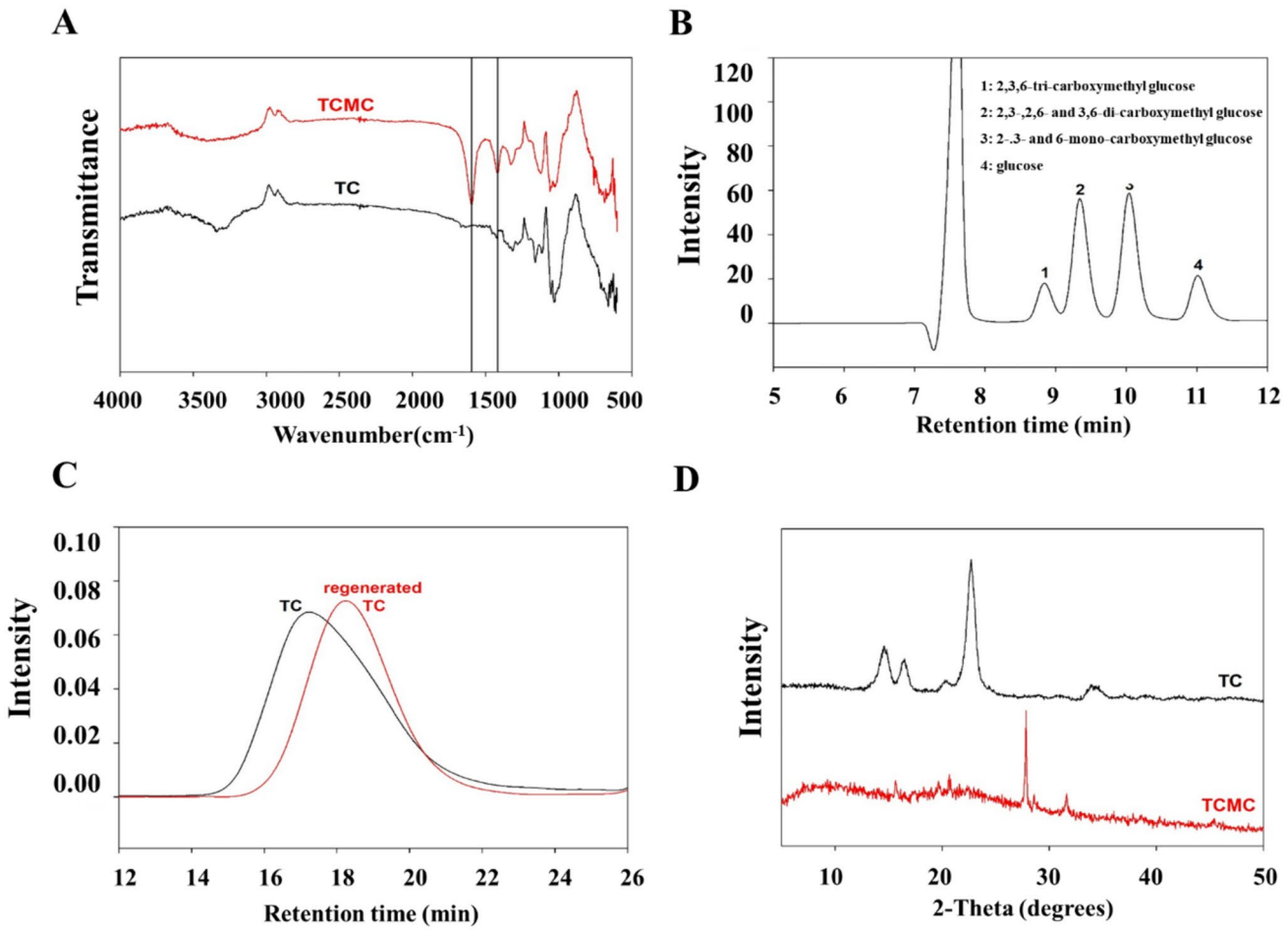

Fig. 2 **A** FT-IR spectra of tunicate cellulose (TC) and tunicate carboxymethyl cellulose (TCMC). **B** HPLC chromatogram of glucose, mono-carboxymethyl glucose, di-carboxymethyl glucose, and tri-carboxymethyl glucose in a hydrolyzed TCMC sample. **C** GPC chromatogram of TC and regenerated TC after dissolution in lithium perchlorate. **D** XRD patterns of TC and TCMC. *FT-IR* Fourier-transform infrared spectroscopy, *HPLC* high-performance liquid chromatography, *GPC* gel permeation chromatography, *XRD* X-ray diffraction

In this study, TC was exclusively and homogeneously carboxymethylated using lithium perchlorate. The carboxymethylation of TC might be hindered by its unique higher MW and excellent crystallinity compared to other forms of cellulose. To mitigate these factors, the MW and crystallinity of TC were decreased by dissolving it in lithium perchlorate.

The alteration in the MW of TC due to dissolution in lithium perchlorate was explored by measuring the MW of regenerated TC after its dissolution in lithium perchlorate (Fig. 2C). The M_n and M_w values of the regenerated TC were 114,606 and 505,938, respectively. These values represent a 70% and 32% reduction in the initial values, respectively. The resulting DP_n and DP_w values of the regenerated TC were 221 and 975, respectively. The PDI value of the regenerated TC also decreased from 9.5 in the original TC to 4.4. The dissolution process of TC in lithium perchlorate substantially diminished the MW of TC while augmenting its uniformity. As a result, the homogeneous dissolution process enhanced the reaction efficiency of carboxymethylation with sodium chloroacetate. The heightened water solubility of TCMC can be partially attributed to reduced internal hydrogen bonding resulting from the lower MW.

TC typically exhibits significantly higher crystallinity compared to other types of cellulose. The high crystalline structure of TC can also limit its functionalization efficiency. Therefore, few functionalization results of TC have been reported. The XRD diagrams of TC showed characteristic peaks of cellulose at 14.6°, 16.6°, 20.5°, 22.8°, and 34.3°. The CrI value of TC calculated from the XRD diagram is 90.1, which is very high compared to other celluloses (Fig. 2D) [6]. The XRD patterns of TCMC showed that the main diffraction peak was shifted and widened at $2\theta = 20.7°$. The existence of peaks at approximately $2\theta = 20°$ suggested the conversion of the crystal structure into an amorphous state [40]. A CrI value for TCMC could not be determined. The homogeneous carboxymethylation process completely

changed the highly crystalline structure of TC into an amorphous state. The high water solubility of TCMC can also be explained by its amorphous structure.

3.3 TCMC ultrasound gel formulation

Ultrasound gel must possess specific physicochemical properties such as viscosity, conductivity, and pH in order for it to effectively transmit signals. Commercial ultrasound gels commonly contain carbopol, triethanolamine, glycerin, and water.

Carbopol is used in biomedical and cosmetic applications due to its thickening, suspending, and stabilizing properties. It comprises polyacrylic acids containing 56%–68% carboxylic acid (–COOH) groups. These groups act as carboxyl donors, forming hydrogen bonds with water molecules. When dispersed in water, carbopol molecules uncoil and increase viscosity, enhancing the gel's performance [15].

Triethanolamine is another key component in ultrasound gel, as it forms crosslinks with carbopol, further increasing viscosity [4]. The U.S. Food and Drug Administration (FDA) has set a maximum standard of triethanolamine around 5% in solution. Above that, the mild skin irritation was observed [10]. Consequently, the concentration of triethanolamine in this study was kept below 3% in solution.

Glycerin, which readily dissolves in water or alcohol, plays a significant role in the gel's intricate conformational dynamics and hydrogen bond networks [51]. Therefore, it influences the swelling and viscoelastic properties of the ultrasound gel [52].

In this study, TCMC was incorporated into a mixture of carbopol, triethanolamine, and glycerin, designated as the 'base gel,' for experimental purposes. The addition of TCMC to the base gel leads to the formation of more intricate polymer networks through both ionic and hydrogen bonds. The resilient fibers of TCMC enhance gel stability, while its dense network accommodates more water molecules, thereby improving wettability and moisture retention [31, 55]. The gel's ability to retain water helps prevent rapid and irreversible dehydration during repeated ultrasonic treatments [29].

3.4 Characterization of the TCMC ultrasound gel

As the gel directly interacts with tissue, it must adhere to specific pH levels corresponding to the targeted tissue conditions. The skin typically maintains a pH of 4.0–7.0, and pH level below 2.0 or above 11.0 is considered corrosive or severely irritating to the skin. Skeletal muscle requires a pH range of approximately 6.9–7.4, while cancerous tissue typically thrives within a pH range of 5.8–6.5. Hence, the pH of the gel should be tailored accordingly for optimal effectiveness in each scenario [17, 24]. The TCMC content in various base gels corresponds to different pH ranges, as presented in the table below (Table 1), and some fall around the pH range suitable for skin application.

Variations in ultrasound gel viscosity directly affect the transmission of vibrations through the skin. Higher viscosity increases fluid flow resistance, slowing down its average velocity [20, 43]. Conversely, lower viscosity encourages faster evaporation, which can hinder the efficient delivery of molecules. Therefore, it is crucial to adjust the gel's viscosity to suit its intended applications, whether for muscle stimulation, imaging, or drug delivery. The recommended viscosity range within therapeutic contexts typically falls between 200 and 800 P (Fig. 3A) [48].

BG2T3 and BG5T3 exhibit viscosities of 434.23 P and 358.53 P, respectively, while the commercial gel has a viscosity of approximately 307.63 P (Fig. 3B). The introduction of TCMC alters the rheological properties of the gel due to its relatively high aspect ratio. TC, featuring fibers 5–10 times longer than those in plants (ranging from 1000 to 2000 nm compared to 200–300 nm), contributes to a more tangled structure, thereby increasing gel stiffness and viscosity [9]. Glycerin, functioning as a plasticizer, reduces chain strength and increases molecular spacing, facilitating movement between TCMC and carbomer molecules. Consequently, the interactions between the molecular chains of both TCMC and carbomer are strengthened. These factors contribute to the observed differences in viscosity between the TCMC gel and the base gel (Fig. 3B, Table 1, Table S1) [53].

Table 1 pH of the examined TCMC gel formulations

Gel name	Base gel	TCMC concentration (%, w/v)	pH
BG1T1	C1T3G1	1	9.37 ± 0.04
BG1T2		2	9.36 ± 0.01
BG1T3		3	9.39 ± 0.01
BG2T1	C2T2G1	1	8.10 ± 0.31
BG2T2		2	9.02 ± 0.05
BG2T3		3	6.00 ± 0.01
BG3T1	C3T1G1	1	8.10 ± 0.30
BG3T2		2	7.94 ± 0.02
BG3T3		3	8.49 ± 0.14
BG4T1	C1T2G2	1	9.25 ± 0.03
BG4T2		2	9.35 ± 0.06
BG4T3		3	5.58 ± 0.12
BG5T1	C2T1G2	1	7.26 ± 0.05
BG5T2		2	8.68 ± 0.01
BG5T3		3	4.87 ± 0.58

Values are presented as mean ± standard deviation

TCMC tunicate carboxymethyl cellulose, *C* carbopol, *T* triethanolamine, and G: glycerin

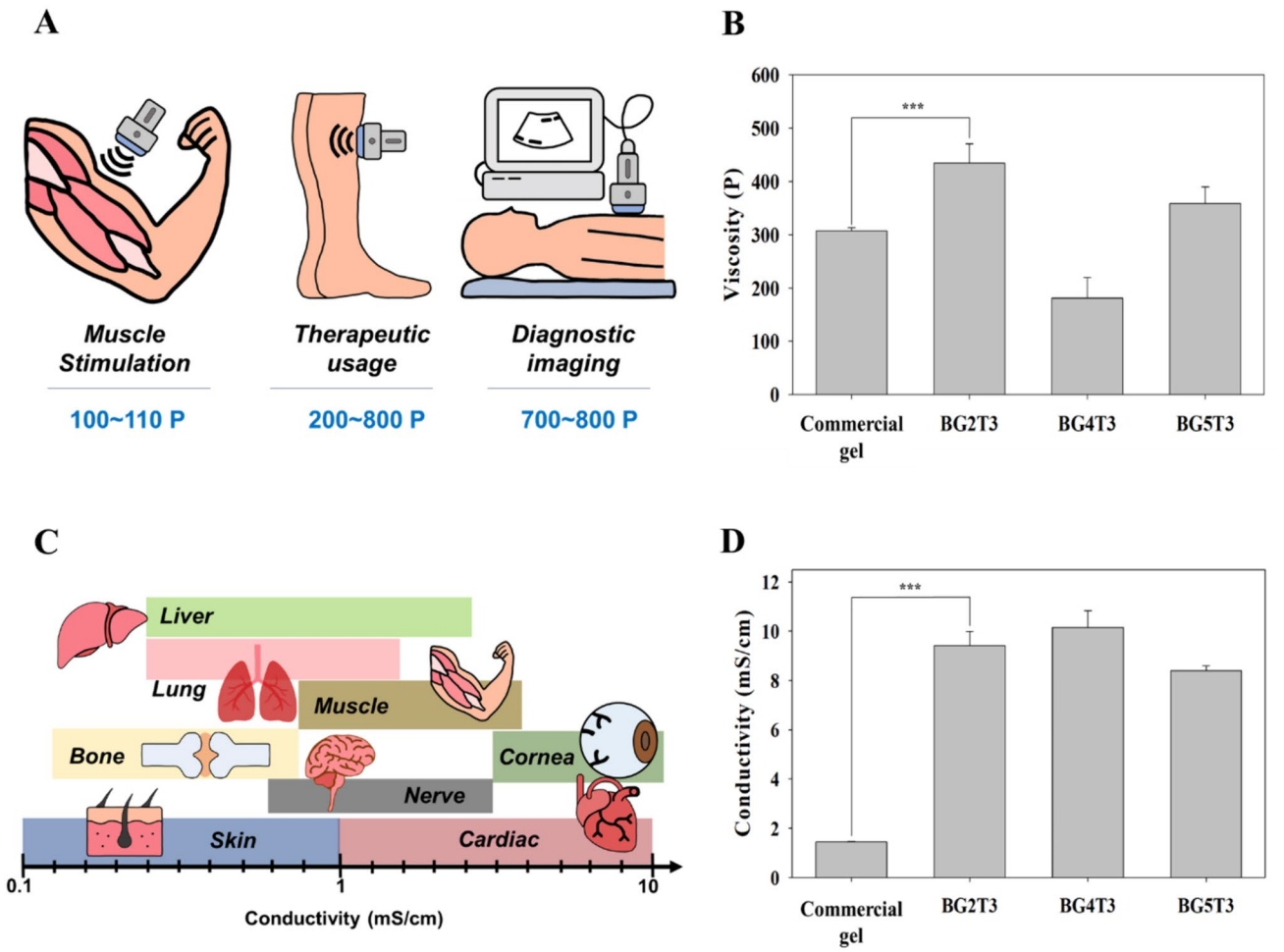

Fig. 3 **A** Ultrasound gel viscosities according to their intended uses. **B** Viscosity of commercial and TCMC gels. **C** Various ranges of tissue conductivity. **D** Conductivity of commercial gel and TCMC gels. TCMC: tunicate carboxymethyl cellulose. All error bars represent the standard deviations ($n = 3$) with statistical significance (***$p < 0.005$)

The abundant hydroxyl groups present in TC confer conductivity to the material and offer numerous reactive sites for the attachment of carboxymethyl groups. TC has an aspect ratio of approximately 80, indicating that its fibers are elonga These findings demonstrate that adding TCMC significantly enhances the gel's conductivity, maintaining relatively stable performance across a broad temperature range with only minor fluctuations. ted and slender. Additionally, TC exhibits a high specific surface area exceeding 15 times that of plants, ranging from 150 to 170 m^2/g, compared to plants, which typically fall around 10 m^2/g [32, 56]. The elevated surface energy and reactivity of TC stem from its abundance of polar groups [47]. Furthermore, the carboxymethylation process introduces potent anionic charges to cellulose, leading to electrostatic repulsion [46]. This repulsion plays an important role in determining the viscosity of the suspension and its water solubility [8]. CMC interacts through electrostatic forces with carbopol and triethanolamine present in the base gel [18]. This CMC enhances electrical properties such as conductivity and improves cellulose-based ultrasound gel's accuracy, precision, and signal transmission [13, 22, 34, 39].

In this study, the conductivity levels of all gel samples were consistent with those found in the therapeutic range for muscle stimulation (Fig. 3C), which typically falls within a 1–10 mS/cm range [36]. Higher proportions of TCMC addition tend to result in more significant increases in gel conductivity. BG2T3, BG4T3, and BG5T3 exhibited conductivity values of 9.41 mS/cm, 10.16 mS/cm, and 8.40 mS/cm, respectively. Conversely, both the commercial and base gel, which do not contain TCMC, exhibited much lower conductivity levels of approximately 1.44 mS/cm, 2.71 mS/cm, 2.47 mS/cm, and 1.13 mS/cm, respectively (Fig. 3D, Table S1). The enhanced conductivity of TCMC-containing gel has important implications for ultrasonic sonophoresis, providing key advantages such as minimal risk of skin damage, the ability to target a wide range of drugs, penetration

depths of approximately 5 cm, and rapid treatment durations [35]. Among the various 3% TCMC gels examined herein, BG2T3 was ultimately selected for further experiments.

3.5 BG2T3 stability analysis

Maintaining consistent pH levels is critical for ensuring the gel's chemical stability, solubility, and electrical conductivity, which is essential for precise signal measurements [1, 42]. A pH mismatch with the skin can compromise the skin barrier and lead to adverse effects. Therefore, it is crucial to maintain pH within the prescribed range under varying environmental conditions. Ensuring viscosity and conductivity is essential to maintaining the gel's stability and achieving consistent ultrasound-assisted molecular delivery. Fluctuations in viscosity or conductivity can lead to unstable ultrasound wavelengths, resulting in abrupt temperature changes that may cause skin burns or irritation [3].

The gel's stability at various temperatures (4 °C, 23 °C, and 50 °C) was confirmed over 7 days by monitoring pH, viscosity, and conductivity (Table 2). The pH was maintained within a 4 to 7 range across all temperatures, confirming that the BG2T3 is compatible and suitable for skin-contacting therapies.

BG2T3 showed narrow viscosity changes compared to the base gel. This stability is likely due to the rigid cellulose chain maintaining its spatial structure and preventing fluctuations in its rheological behavior [2]. Increasing the DS enhances the molecular charge density, leading to a stabilization effect by surpassing the ion-binding capacity. The degree of polymerization and the viscosity of CMC are largely determined by its average chain length and DS [7], with the longer chain lengths and higher DS of TCMC providing stable viscosity. The addition of TCMC also contributes to stabilizing changes in gel conductivity. The conductivity of BG2T3 varied by less than 20% across temperatures (19.02% at 4 °C, 7.76% at 23 °C, and 1.48% at 50 °C), while the base gel exhibited rapid decreases in conductivity of more than 30% (35.66% at 4 °C, 68.01% at 23 °C, and 55.51% at 50 °C). These findings demonstrate that adding TCMC significantly enhances the gel's conductivity, maintaining relatively stable performance across a broad temperature range with only minor fluctuations.

3.6 Small molecule delivery with BG2T3-mediated ultrasound

The cavitation effect occurring within the ultrasound gel facilitates the destruction of microbubbles, thereby enhancing the drug release capability. This cavitation effect, responsive to ultrasound energy, allows for effective therapies by stably collapsing microbubbles [49]. Moreover, drug release induced by ultrasound stimulation offers several key advantages, such as controlled drug release from drug delivery carriers, enabling modulation of drug release quantity, absorption, and disease targeting within the body [11]. Accurately regulating drug release has several advantages such as reduced side effects, improved therapeutic efficacy, and enhanced usability [23].

The MW of brilliant blue (854.02 g/mol) contained in the gel is similar to that of the anticancer drug Taxol (854 g/mol). It is comparable to other antiviral agents such as Crixivan (712 g/mol) and the aminoglycoside antibiotic gentamicin (694.7 g/mol) [37]. An ultrasound-based dye molecule delivery system (Fig. 4A) was established to assess the dye molecule dispersal capability of the ultrasound gel, and the dye diffusion of BG2T3 was examined. The results showed that dye release began after the ultrasound treatment, gradually increased, and reached a 54.06% release rate at 11 min (Fig. 4B).

Despite being fast and straightforward, ultrasound therapy poses burn risks due to the self-heating of the device using ultrasound waves, highlighting the need for rapid molecule release. In previous studies, cellulose hydrogel demonstrated increased nicotine release upon the application of ultrasound, releasing over 50% of nicotine within an hour. Another cellulose hydrogel demonstrated 50% propionic acid and butyrate release within 20 min [19, 54]. BG2T3 achieved 50% dye release in 11 min, significantly faster than the two hydrogel examples discussed above. Thus, the TCMC exhibited a promising molecular delivery ability

Table 2 The pH, viscosity, and conductivity changes of the gel after 7 days

		Before incubation	After incubation temperature (°C)		
			4	23	50
BG2T3	pH	6.00 ± 0.01	5.47 ± 0.12	6.61 ± 0.23	6.43 ± 0.12
	Viscosity (P)	434.23 ± 36.55	456.40 ± 8.41	507.66 ± 30.11	587.73 ± 55.31
	Conductivity (mS/cm)	9.41 ± 0.57	7.62 ± 2.27	8.68 ± 1.04	9.55 ± 1.74
Base gel	pH	5.58 ± 0.12	6.68 ± 0.08	7.20 ± 0.09	6.89 ± 0.04
	Viscosity (P)	525.01 ± 30.41	891.63 ± 11.77	833.76 ± 9.34	904.23 ± 52.10
	Conductivity (mS/cm)	2.72 ± 0.17	1.75 ± 0.20	0.87 ± 0.04	1.21 ± 0.01

Values are presented as mean ± standard deviation

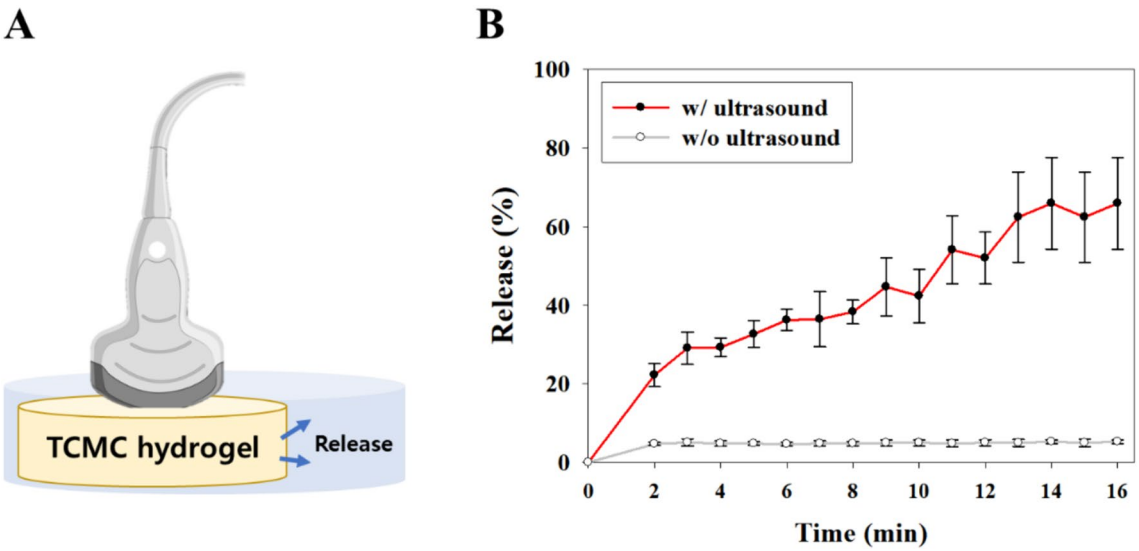

Fig. 4 **A** Ultrasound transmission through the dermal layer (image from BioRender). **B** Release of dye molecule from BG2T3. TCMC: tunicate carboxymethyl cellulose

and increased conductivity, especially when combined with ultrasound.

4 Conclusion

Ultrasound gels are tailored for specific use ranges. This study utilized a material derived from tunicate by-products (TS) to produce ultrasound gel. Cellulose extracted from TS was then synthesized with carboxymethyl groups to enhance solubility and wettability. This synthesized material was formulated into ultrasound gel using thickening polymers such as carbopol, glycerin, and triethanolamine. Various formulations of ultrasound gels were assessed for pH, viscosity, and conductivity to optimize conditions suitable for transdermal therapy. Among these formulations, BG2T3 exhibited favorable characteristics, particularly high conductivity attributed to the ionization of carboxymethyl groups. Therefore, the gel that has been developed holds promise as a prospective candidate for ultrasound-based drug release systems.

Supplementary Information The online version contains supplementary material available at https://doi.org/10.1007/s12257-024-00146-x.

Acknowledgements This work was supported by the technology development for biomaterialization of marine fisheries byproducts (KIMST-20220128) of the Korea Institute of Marine Science & Technology Promotion (KIMST), funded by the Ministry of Oceans and Fisheries, Korea.

Declarations

Conflict of interest The authors declare no conflict of interest.

Ethical approval Neither ethical approval nor informed consent was required for this study.

References

1. Afzal S, Zahid M, Rehan ZA et al (2022) Preparation and evaluation of polymer-based ultrasound gel and its application in ultrasonography. Gels 8:42. https://doi.org/10.3390/gels8010042
2. Armoškaitė V, Ramanauskienė K, Briedis V (2012) Evaluation of base for optimal drug delivery for iontophoretic therapy: Investigation of quality and stability. Afr J Pharm Pharmacol 6:1685–1695. https://doi.org/10.5897/AJPP12.208
3. Bai W, Kong L, Guo A (2013) Effects of physical properties on electrical conductivity of compacted lateritic soil. J Rock Mech Geotech Eng 5:406–411. https://doi.org/10.1016/j.jrmge.2013.07.003
4. Berardi A, Perinelli DR, Bisharat L et al (2022) Factors affecting the rheological behaviour of carbomer dispersions in hydroalcoholic medium: towards the optimization of hand sanitiser gel formulations. Int J Pharm 616:121503. https://doi.org/10.1016/j.ijpharm.2022.121503
5. Chanthathamrongsiri N, Petchsomrit A, Leelakanok N et al (2021) The comparison of the properties of nanocellulose isolated from colonial and solitary marine tunicates. Heliyon 7:e07819. https://doi.org/10.1016/j.heliyon.2021.e07819
6. Cheng Y, Mondal AK, Wu S et al (2020) Study on the anti-biodegradation property of tunicate cellulose. Polymers (Basel) 12:3071. https://doi.org/10.3390/polym12123071
7. Ding H, Hou R, Li Y et al (2020) Effect of different carboxymethyl cellulose structure parameters on tartrates stability of red wine: viscosity and degree of substitution. Food Addit Contam Part A 37:1099–1109. https://doi.org/10.1080/19440049.2020.1755062
8. Dunlop MJ, Clemons C, Reiner R et al (2020) Towards the scalable isolation of cellulose nanocrystals from tunicates. Sci Rep 10:19090. https://doi.org/10.1038/s41598-020-76144-9

9. Dunlop MJ, Acharya B, Bissessur R (2020) Study of plant and tunicate based nanocrystalline cellulose in hybrid polymeric nanocomposites. Cellulose 27:249–261. https://doi.org/10.1007/s10570-019-02791-5
10. Fiume MM, Heldreth B, Bergfeld WF et al (2013) Safety assessment of triethanolamine and triethanolamine-containing ingredients as used in cosmetics. Int J Toxicol 32:595–835
11. Freiberg S, Zhu XX (2004) Polymer microspheres for controlled drug release. Int J Pharm 282:1–18. https://doi.org/10.1016/j.ijpharm.2004.04.013
12. Fu J, Pang Z, Yang J et al (2015) Fabrication of polyaniline/carboxymethyl cellulose/cellulose nanofibrous mats and their biosensing application. Appl Surf Sci 349:35–42. https://doi.org/10.1016/j.apsusc.2015.04.215
13. Gonzalez-Macia L, Morrin A, Smyth MR et al (2010) Advanced printing and deposition methodologies for the fabrication of biosensors and biodevices. Analyst 135:845–867. https://doi.org/10.1039/B916888E
14. Hebeish A, Hashem M, El-Hady MM et al (2013) Development of CMC hydrogels loaded with silver nano-particles for medical applications. Carbohydr Polym 92:407–413. https://doi.org/10.1016/j.carbpol.2012.08.094
15. Houlleberghs M, Verheyden L, Voorspoels F et al (2023) Magneto-hydrodynamic mixing: a new technique for preparing carbomer hydrogels. AIChE J 69:e17911. https://doi.org/10.1002/aic.17911
16. Hubbell CA, Ragauskas AJ (2010) Effect of acid-chlorite delignification on cellulose degree of polymerization. Bioresour Technol 101:7410–7415. https://doi.org/10.1016/j.biortech.2010.04.029
17. Hwang JH, Lee S, Lee HG et al (2022) Evaluation of skin irritation of acids commonly used in cleaners in 3D-reconstructed human epidermis model. KeraSkin™ Toxics 10:558. https://doi.org/10.3390/toxics10100558
18. Iglesias N, Galbis E, Romero-Azogil L et al (2020) In-depth study into polymeric materials in low-density gastroretentive formulations. Pharmaceutics 12:636. https://doi.org/10.3390/pharmaceutics12070636
19. Iresha H, Kobayashi T (2021) Ultrasound-triggered nicotine release from nicotine-loaded cellulose hydrogel. Ultrason Sonochem 78:105710. https://doi.org/10.1016/j.ultsonch.2021.105710
20. Kawabata Y (2012) Effect of coefficient of viscosity and ambient temperature on the flow rate of drug solutions in infusion pumps. Pharm Dev Technol 17:755–762. https://doi.org/10.3109/10837450.2011.583926
21. Kim S, Song M, Lee M et al (2023) Controlled release of quercetin from HPMC/gellan gum hydrogel for inhibiting melanogenesis in murine melanoma cells. Korean J Chem Eng 40:337–343. https://doi.org/10.1007/s11814-022-1269-y
22. Kiran Raj G, Singh E, Hani U et al (2023) Conductive polymers and composites-based systems: an incipient stride in drug delivery and therapeutics realm. J Control Release 355:709–729. https://doi.org/10.1016/j.jconrel.2023.02.017
23. Kubota T, Kurashina Y, Zhao J et al (2021) Ultrasound-triggered on-demand drug delivery using hydrogel microbeads with release enhancer. Mater Des 203:109580. https://doi.org/10.1016/j.matdes.2021.109580
24. Lambers H, Piessens S, Bloem A et al (2006) Natural skin surface pH is on average below 5, which is beneficial for its resident flora. Int J Cosmet Sci 28:359–370. https://doi.org/10.1111/j.1467-2494.2006.00344.x
25. Lebaz N, Cockx A, Spérandio M et al (2015) Population balance approach for the modelling of enzymatic hydrolysis of cellulose. Can J Chem Eng 93:276–284. https://doi.org/10.1002/cjce.22088
26. Lee JH, Lim SJ, Oh DH et al (2010) Wound healing evaluation of sodium fucidate-loaded polyvinylalcohol/sodium carboxymethylcellulose-based wound dressing. Arch Pharm Res 33:1083–1089. https://doi.org/10.1007/s12272-010-0715-2
27. Li H, Shi H, He Y et al (2020) Preparation and characterization of carboxymethyl cellulose-based composite films reinforced by cellulose nanocrystals derived from pea hull waste for food packaging applications. Int J Biol Macromol 164:4104–4112. https://doi.org/10.1016/j.ijbiomac.2020.09.010
28. Li CH, Chang YC, Hsiao M et al (2022) Ultrasound and nanomedicine for cancer-targeted drug delivery: screening, cellular mechanisms and therapeutic opportunities. Pharmaceutics 14:1282. https://doi.org/10.3390/pharmaceutics14061282
29. Lionetto F, Sannino A, Maffezzoli A (2005) Ultrasonic monitoring of the network formation in superabsorbent cellulose based hydrogels. Polym 46:1796–1803. https://doi.org/10.1016/j.polymer.2005.01.008
30. Liu H, Sale KL, Holmes BM et al (2010) Understanding the interactions of cellulose with ionic liquids: a molecular dynamics study. J Phys Chem B 114:4293–4301. https://doi.org/10.1021/jp9117437
31. Liu Y, Li S, Wang Z et al (2022) Ultrasound in cellulose-based hydrogel for biomedical use: from extraction to preparation. Colloids Surf B Biointerfaces 212:112368. https://doi.org/10.1016/j.colsurfb.2022.112368
32. Lu P, Hsieh YL (2010) Preparation and properties of cellulose nanocrystals: rods, spheres, and network. Carbohydr Polym 82:329–336. https://doi.org/10.1016/j.carbpol.2010.04.073
33. Lv X, Han J, Liu M et al (2023) Overview of preparation, modification, and application of tunicate-derived nanocellulose. Chem Eng J 452:139439. https://doi.org/10.1016/j.cej.2022.139439
34. Ma Z, Zhou Y, Cai F et al (2020) Ultrasonic microstreaming for complex-trajectory transport and rotation of single particles and cells. Lab Chip 20:2947–2953. https://doi.org/10.1039/D0LC00595A
35. Mitragotri S, Blankschtein D, Langer R (1996) Transdermal drug delivery using low-frequency sonophoresis. Pharm Res 13:411–420. https://doi.org/10.1023/a:1016096626810
36. Munawar MA, Schubert DW (2022) Thermal-induced percolation phenomena and elasticity of highly oriented electrospun conductive nanofibrous biocomposites for tissue engineering. Int J Mol Sci 23:8451. https://doi.org/10.3390/ijms23158451
37. Nauck MA, Quast DR, Meier JJ (2021) Another milestone in the evolution of GLP-1-based diabetes therapies. Nat Med 27:952–953. https://doi.org/10.1038/s41591-021-01394-7
38. Neri TAN, Palmos GN, Park SY et al (2022) Hair growth-promoting activities of glycosaminoglycans extracted from the tunics of ascidian (*Halocynthia roretzi*). Polymers (Basel) 14:1096. https://doi.org/10.3390/polym14061096
39. Nyborg WL (1982) Ultrasonic microstreaming and related phenomena. Br J Cancer Suppl 5:156–160
40. Park S, Oh Y, Jung D et al (2020) Effect of cellulose solvents on the characteristics of cellulose/Fe_2O_3 hydrogel microspheres as enzyme supports. Polymers 12:1869. https://doi.org/10.3390/polym12091869
41. Pitt WG, Husseini GA, Staples BJ (2004) Ultrasonic drug delivery–a general review. Expert Opin Drug Deliv 1:37–56. https://doi.org/10.1517/17425247.1.1.37
42. Polat BE, Hart D, Langer R et al (2011) Ultrasound-mediated transdermal drug delivery: mechanisms, scope, and emerging trends. J Control Release 152:330–348. https://doi.org/10.1016/j.jconrel.2011.01.006
43. Salmon M, Salmon C, Bissinger A et al (2015) Alternative ultrasound gel for a sustainable ultrasound program: application of human centered design. PLoS ONE 10:e0134332. https://doi.org/10.1371/journal.pone.0134332

44. Schlufter K, Heinze T (2010) Carboxymethylation of bacterial cellulose. Macromol Symp 294:117–124. https://doi.org/10.1002/masy.200900054
45. Schroeder LR, Gentile VM, Atalla RH (1986) Nondegradative preparation of amorphous cellulose. J Wood Chemi Technol 6:1–14. https://doi.org/10.1080/02773818608085213
46. Shak KPY, Pang YL, Mah SK (2018) Nanocellulose: recent advances and its prospects in environmental remediation. Beilstein J Nanotechnol 9:2479–2498. https://doi.org/10.3762/bjnano.9.232
47. Singh R, Kumar S (2022) Cancer targeting and diagnosis: recent trends with carbon nanotubes. Nanomaterials 12:2283. https://doi.org/10.3390/nano12132283
48. Society of Radiographers and British Medical Ultrasound Society (2017) Guidelines for professional ultrasound practice. Revision 2. Society of Radiographers and British Medical Ultrasound Society, London
49. Tharkar P, Varanasi R, Wong WSF et al (2019) Nano-enhanced drug delivery and therapeutic ultrasound for cancer treatment and beyond. Front Bioeng Biotechnol 7:324. https://doi.org/10.3389/fbioe.2019.00324
50. Thümmler K, Fischer S, Peters J et al (2010) Evaluation of molten inorganic salt hydrates as reaction medium for the esterification of cellulose. Cellulose 17:161–165. https://doi.org/10.1007/s10570-009-9344-7
51. Towey JJ, Dougan L (2012) Structural examination of the impact of glycerol on water structure. J Phys Chem B 116:1633–1641. https://doi.org/10.1021/jp2093862
52. Varges PR, Costa CM, Fonseca BS et al (2019) Rheological characterization of Carbopol® dispersions in water and in water/glycerol solutions. Fluids 4:3. https://doi.org/10.3390/fluids4010003
53. Xu D, Cheng Y, Wu S et al (2022) Study on the effect of tunicate cellulose nanocrystals in the preparation of sodium alginate-based enteric capsule. Cellulose 29:2497–2511. https://doi.org/10.1007/s10570-022-04445-5
54. Yan L, Wang L, Gao S et al (2020) Celery cellulose hydrogel as carriers for controlled release of short-chain fatty acid by ultrasound. Food Chem 309:125717. https://doi.org/10.1016/j.foodchem.2019.125717
55. Yao K, Li S, Zheng X et al (2024) Superwettable calcium ion exchanged carboxymethyl cellulose powder with self-gelation, tissue adhesion and bioabsorption for effective hemorrhage control. Chem Eng J 481:148770. https://doi.org/10.1016/j.cej.2024.148770
56. Zhao Y, Zhang Y, Lindström ME et al (2015) Tunicate cellulose nanocrystals: preparation, neat films and nanocomposite films with glucomannans. Carbohydr Polym 117:286–296. https://doi.org/10.1016/j.carbpol.2014.09.020
57. Zhao Y, Moser C, Henriksson G (2018) Transparent composites made from tunicate cellulose membranes and environmentally friendly polyester. Chemsuschem 11:1728–1735. https://doi.org/10.1002/cssc.201800627